Journal of Applied Research on Industrial Engineering
www.journal-aprie.com

Modelling and Analysis of 2-Stage Planetary Gear Train for Modular Horizontal Wind Turbine Application

Aniekan Essienubong Ikpe [1,*], Ekom Mike Etuk[2], Azum Uwarisi Adoh[3]

[1]*Department of Mechanical Engineering, University of Benin, Benin City, Nigeria.*
[2]*Department of Production Engineering, University of Benin, Benin City, Nigeria.*
[3]*National Board of Technology Incubation, Warrior, Delta State, Nigeria.*

PAPER INFO

Chronicle:
Received: 24 July 2019
Revised: 11 October 2019
Accepted: 04 December 2019

Keywords:
Modeling.
Planetary gear.
Wind turbine.
Stress.
Strain.
Deformation.
FOS.

ABSTRACT

Wind turbine incorporates a gear box which aids the transmission of torque for the generation of wind energy, industry professionals have streamlined the gearbox design to suite this purpose. Despite the advancement in the gear box design, most wind turbine downtime is attributed to gearbox-related problems. In this study, Finite Element Method through ANSYS R15.0 software was employed in modelling and analysis of a 2-stage planetary gear train for modular horizontal wind turbine. The ring gear was considered as statically constrained member because it is practically fixed to the gearbox housing while the dynamics of the planet gear, planet carrier and the sun pinion were considered as rotating members. Using Factor of Safety (FOS) ranging from 10-15, the gear model was simulated to determine the equivalent stresses, strains and total deformation. The simulation which was conducted for five (5) steps at 2.5 seconds each yielded minimum and maximum Von-mises stress of 10.168 Pa and 5.9889e+009 Pa for the 5th step, minimum and maximum equivalent elastic strain of 5.0839e-011 and 2.9944e-002 for the 5th step and maximum total deformation of 1.7318e-003 m at the 5th step. The findings revealed that the higher the design FOS, the lower the stress-strain deformations, indicating longevity and optimum performance of the gear system. It was observed that increase in contact forces between the meshing gear teeth may cause larger elastic deformations, increasing tooth bending deformation as well as larger backlash on the gear teeth while continuously varying gear mesh stiffness with time can result in excessive vibration and noise.

1. Introduction

Planetary Gears, despite the various capacities and ratings are one of the most widely used mechanical component that fits into several industrial applications. Due to its higher efficiency, high torque density, higher feasible gear ratios, compactness, light weight and high load bearing capacity, planetary gear plays a vital role in several mechanical applications such as electric screwdrivers, automatic transmission in vehicles, bicycle hubs and wind turbine gear boxes which is the point of focus in this study [1]. The design service life of a simple wind turbine system is over 20 years, but the gearboxes which converts the rotor blade rotational speed between 5 and 22 rpm to the generator required rotational speed of about 1600-1800 rpm typically fall within operational period of 5 years [2]. Planetary gear trend also known as epicyclic gear trains consist of gear system that one or more gears orbit about

* Corresponding author
E-mail address: alwaysetuk@gmail.com
DOI: 10.22105/jarie.2020.213154.1114

the central axis of the train. The fact that planetary gears have moving axes makes them complex and different from ordinary trains. The primary purpose of a planetary gear in mechanical systems is to minimise the rotating speed in order to generate higher torque. In other words, it transforms the rate of a rotating moment into slower rotating rate to produce higher force or faster rotating rate to produce lower force.

Cooley and Parker [3] carried out an extensive review on planetary gear dynamics and vibrations. The findings obtained from models on forced response of planetary gears showed resonances from mesh stiffness fluctuations and nonlinearity as a result of tooth separation. Moreover, experiments on planetary gears also indicated that complex phenomena such as elastic gear vibration can occur during operation of the gear train. Finally, the authors suggested that tooth surface modifications which are applicable to almost all gears should be designed using system planetary gear models rather than isolated sun-planet and ring-planet gear pair models. Hohn et al. [4] presented a comprehensive Design on Light-weight Planetary gear transmissions and found that a higher number of applied planet gears may result in higher mesh load factor while planets with low numbers of teeth may pose challenges during assembling. As a result of that, the number of teeth for the central gears is increased in order to compensate for adequate power division for higher numbers of applied planets. Hamand and Kalamkar [5] investigated the stresses and deflection in sun gear tooth of planetary gearbox applicable to Grabbing Crane, and observed an appreciable reduction in bending and shear stress value for trochoidal root fillet design compared to stress values in circular root fillet design. An increase was observed in wear stress value for trochoidal root fillet design compared to that of stress values in circular root fillet design, and deflection in trochoidal root fillet was observed to be less compared to that of circular root fillet gear tooth. Pawar and Kulkarni [6] designed a two-stage planetary gear train for high reduction ratio. Reduction ratio of 78:1 was achieved for the two stage planetary gears which was in 3 stage for helical gears. The findings revealed that planetary gears have higher torque density and offers more uniform strength in bending than helical gears. This report covers the modelling and analysis of 2-stage planetary gear train in wind turbine to determine the effects of its duty cycle on the overall performance of the gear system.

2. Materials and Methods

As shown in Fig. 1, the planetary gear train presented in this study was modelled using ANSYS R15.0, while Finite Element Method (FEM) was employed in the simulation of the gear models. The planetary gear train is made up of two or more gears assembled such that the center of one gear rotates around the center of the others. This includes a centrally pivoted sun gear which represents the central gear, planet gear which represents peripheral gears of the same size meshed with the sun gear while annulus or planet carrier supports one or more peripheral planet gears of the same size meshed with the sun gear and the ring gear/annulus is an outer ring with inward-facing teeth that mesh with the planet gears. As shown in Figure 1a, the planet carrier ensures that proper planet gear and sun gear center distances are maintained. Vibrational effects are transmitted to the planet carrier which distributes torsional load among the planet gears such that their interaction with the sun gear can be effective. Operating principle of the planetary gear train is such that, the planet and sun gear mesh in order to allow their pitch circles roll without slip. Amidst this process, there is also an interplay between the planets, the ring gear (which is fixed to the inertial frame) and the sun gear (which is constrained to the reference frame but allowed to rotate). For power generation, the central shaft is connected to the wind turbine generator which converts the rotary motion of the output shaft into electrical power. Structural steel (S45C Carbon steel containing about 0.45% carbon) was selected for the gear material due to its high strength to weight ratio and flexibility, and the material properties from ANSYS material library is presented in Table 1.

As indicated with red arrow in Figure 1b, the service operation of the planetary gear is characterized by clockwise motion (+ive) while the motions applicable to the second stage planetary gear are presented in Table 2.

Table 1. *Material properties of the planetary gear.*

Properties	Values	Properties	Values
Density	*7850 kg m^-3*	*Strength Coefficient*	*9.2e+008 Pa*
Coefficient of Thermal Expansion	*1.2e-005 C^-1*	*Strength Exponent*	*-0.106*
Shear Modulus	*7.6923e+010*	*Ductility Coefficient*	*0.213*
Thermal Conductivity	*60.5 W m^-1 C^-1*	*Ductility Exponent*	*-0.47*
Poisson's Ratio	*0.3*	*Cyclic Strength Coefficient*	*1.e+009 Pa*
Compressive Yield Strength	*2.5e+008 Pa*	*Cyclic Strain Hardening Exponent*	*0.2*
Tensile Yield Strength	*2.5e+008 Pa*	*Relative Permeability*	*10000*
Tensile Ultimate Strength	*4.6e+008 Pa*	*Resistivity*	*1.7e-007 ohm m*
Young's Modulus	*2.e+011 Pa*	*Specific Heat*	*434 J kg^-1 C^-1*
Bulk Modulus	*1.6667e+011 Pa*	*Environment Temperature*	*22 °C*

Table 2. *Motions applicable to the second stage.*

Actions	**Clockwise motion +ive**			
	L Speed	**A Speed**	**P Speed**	**S Speed**
Turn the whole train through 1 revolution	*1*	*1*	*1*	*1*
Fix arm L and rotate A back CCW by 1 rev	*0*	*-1*	*$-N_A/N_P$*	*N_A/N_S*
Add the two motions above	*1*	*0*	*$1-(N_A/N_P)$*	*$1+N_A/N_S$*

The output speed and torque of the first stage is equal to the input speed and torque of the second stage neglecting loses over the shaft. The forces considered in the analysis are as follows;

- A constant rotational Force (Torque) of 135Nm was applied to the input Shaft.
- A constant Angular Velocity of 120RPM.

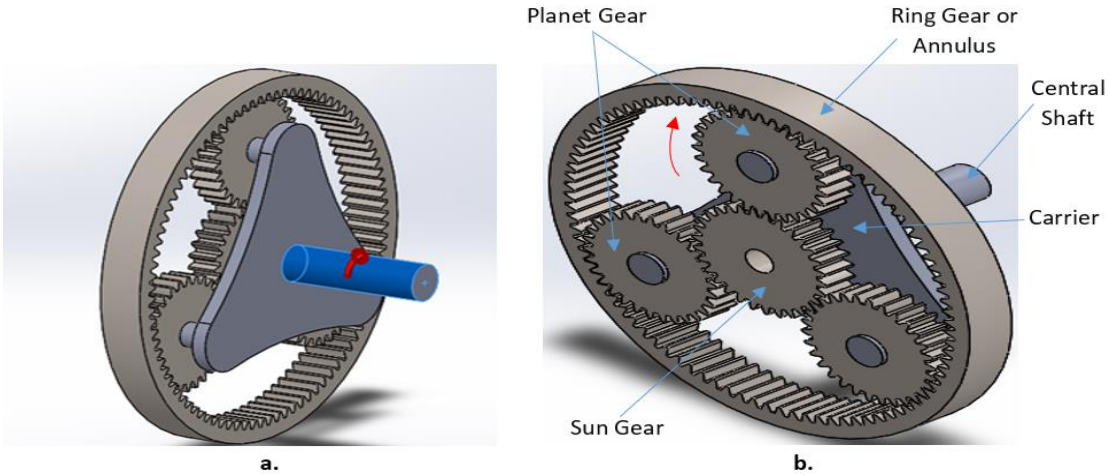

Fig. 1. *Pictorial views of the planetary gear train.*

Gear ratio of the planetary gear is given by Eq. (1);

$$\frac{n_{Hss}}{n_{Lss}} = 1 + \frac{D_{Ring}}{D_{Sun}} \tag{1}$$

Where, n_{Hss} is the rotational speed of the high-speed shaft or output shaft, n_{Lss} is the rotational speed of the low-speed shaft or input input, D_{Ring} is the pitch diameter of the ring or its number of teeth, and D_{Sun} is the pitch diameter of the sun [7].

The velocity ratio mv of the planetary gear is expressed in Eq. (2), with the angular velocity input ω_{in} and the angular velocity output ω_{out} which also can be related to both of the gear-pitch radii.

$$mv = \frac{\omega_{out}}{\omega_{in}} = \pm\frac{r_{in}}{r_{out}} \tag{2}$$

The torque ratio or mechanical advantage ma is the reciprocal of the velocity ratio expressed in Eq.(3);

$$ma = \frac{1}{mv} = \frac{\omega_{in}}{\omega_{out}} \pm \frac{r_{out}}{r_{in}} \tag{3}$$

For the purpose of calculation, the magnitude of the velocity ratio M_G is expressed as the gear ratio [8].

$$m_G = |mv| \text{ or } m_G = |ma| \text{ for } m_G \geq 1 \tag{4}$$

In terms of power P and the pitch circle velocity V_{pitch}, tangential force can be considered in Eq. (5) as one of the loading modes on the tooth gear.

$$F_t = \frac{P}{V_{pitch}} \tag{5}$$

The bending stress on a gear tooth of width b and height h can be determined by applying the bending equation for a cantilevered beam, expressed in Eq. (6). The moment, M, in Eq. 6 is based on a load F_b applied at a distance, L, to the weakest point on the gear tooth. Eq. (6) can be rewritten as express in Eq. (7).

$$\sigma_b = \frac{6M}{bh^2} \tag{6}$$

$$\sigma_b = \frac{F_b}{b}\frac{6L}{h^2} \tag{7}$$

Lewis equation can also be employed in estimating the bending stresses on a gear tooth. In this case, Lewis equation (see Eq. 8) models a gear tooth by taking full load at its tip as a simple cantilever beam.

$$\sigma_b = \frac{Wt\,Pd}{FY} = \frac{Wt\,\pi}{mFY} \tag{8}$$

Where, *Wt* is the tangential load, *Pd* is the diametral pitch, *F* is the face width, *Y* is the Lewis form factor and *m* is the module.

The effective spring constant, k_g, of two meshing gear teeth plays a vital role in the dynamic response (natural frequency) of a wind turbine drive train, and can be expressed in the following relationship;

$$\mathrm{k_g} = \frac{\mathrm{b}}{9}\frac{\mathrm{E_1 E_2}}{\mathrm{E_1 + E_2}} \tag{9}$$

Where, E_1 and E_2 are moduli of elasticity of the gear material.

The helix angle deviation for tooth contact sun/planet can be determined from Equation (10), while the helix angle deviation for tooth contact planet/ring gear (Schulze et al., 2010) [9] can be determined from Eq. (11);

$$\mathrm{FLKM_{1/2}} = \mathrm{ve_1} + \mathrm{ve_{2_{1/2}}} + \mathrm{ve_{WL1/2}} + \mathrm{ve_{PT1/2}} + \mathrm{verkipp_{PL1/2}} + \mathrm{f_{H\beta eff1/2}} \tag{10}$$

$$\mathrm{FLKM_{2/3}} = \mathrm{ve_{2_{2/3}}} + \mathrm{ve_3} + \mathrm{ve_{WL2/3}} + \mathrm{ve_{PT2/3}} + \mathrm{verkipp_{PL2/3}} + \mathrm{f_{H\beta eff2/3}} \tag{11}$$

Where, ve_1 deformation difference of sun, ve_2 deformation difference of planet, ve_3 deformation difference of ring gear, β is the helix angle. The equation of motion for the planetary gear trend [2] is given by Eq. (12);

$$\left(2 + \frac{\mathrm{N_{sun}}}{\mathrm{N_{planet}}}\right)\omega_{\mathrm{annulus}} + \frac{\mathrm{N_{sun}}}{\mathrm{N_{planet}}}\omega_{\mathrm{sun}} - 2 * \left(1 + \frac{\mathrm{N_{sun}}}{\mathrm{N_{planet}}}\right)\omega_{\mathrm{annulus}} = 0 \tag{12}$$

Where, ω_{sun}, $\omega_{annulus}$ and ω_{planet} are the angular velocities of the planetary gear. Since angular velocity of the gear trend during operation is directly proportional to the gear rotation speed in revolution per minute (RPM), Eq. (12) is simplified in Eq. (13) as follows;

$$\left(2 + \frac{\mathrm{N_{sun}}}{\mathrm{N_{planet}}}\right)\mathrm{RPM_{annulus}} + \frac{\mathrm{N_{sun}}}{\mathrm{N_{planet}}}\mathrm{RPM_{sun}} = 2 * \left(1 + \frac{\mathrm{N_{sun}}}{\mathrm{N_{planet}}}\right)\mathrm{RPM_{planet}} \tag{13}$$

3. Results and Discussion

Taken at different points, the moment of inertia which represents the tendency of the rotating gears to resist angular acceleration and the principal axis of inertia representing the axis passing through centroid or centre of gravity of the gears are Tabulated in Table 3.

Table 3. *Moment of inertia and principal axis of inertia of the gear train.*

Moments of inertia and Principal axis of inertia taken at the centre of mass (g/mm^2)		**Moment of Inertia taken at the center of mass and aligned with the output coordinate system (g/mm^2)**		**Moment of Inertia taken at the output coordinate system (g/mm^2)**	
Ix	*0.00, -0.01, 1.00*	*Lxx*	*202603620.33*	*Ixx*	*519635452.75*
Iy	*1.00, -0.02, 0.00*	*Lyx*	*-23865.19*	*Iyx*	*66611113.58*
Iz	*0.02, 1.00, 0.01*	*Lzx*	*-19510.54*	*Izx*	*128195358.89*
Principal axes of inertia		*Lxy*	*-23865.19*	*Ixy*	*66611113.58*
Px	*43321697.08*	*Lyy*	*204171602.61*	*Iyy*	*519641528.30*
Py	*202603257.18*	*Lzy*	*-1307521.15*	*Izy*	*128418815.23*
Pz	*204182596.72*	*Lxz*	*-19510.54*	*Ixz*	*128195358.89*
		Lyz	*-1307521.15*	*Iyz*	*128418815.23*
		Lzz	*43332328.04*	*Izz*	*176611437.93*

Prior to the introduction of gears, wheels were employed in transferring the rotation of one shaft to another through friction. The primary challenge associated with these frictional wheels was slippage beyond a certain torque value due to reduction in the maximum transmitted torque by the frictional torque. This led to the application of tooth wheels also referred to as cogwheels or gears in attempt to overcome this drawback in wheels which manifests as slippage. In gearing systems, the process whereby the teeth of one gear are inserted between the teeth of the mating gear is known as gear meshing. This is the reason why the stiffness of a gear mesh is relevant when accurate understanding of the dynamics and vibration of gearing systems are required. Fig. 2 represents a plot of the planetary gear mesh stiffness with time. As shown in the plot, the gear mesh stiffness varies sinusoidally with the gear teeth meshing time. As represented in the plot, some gear mesh stiffness values are lower while some are higher. This is because at certain meshing points, only one, two or three pairs of teeth are in contact which yields the higher and lower values depending on the meshing effectiveness of the gear teeth. The gear mesh stiffness depends upon a number of parameters, most importantly the gear rotation, and very high gear mesh stiffness with time signifies difficulty in rotation of the gear wheels which can result in increase in vibration, wear rate, noise level as well as stress in different parts of the transmission system due to wear allowance developed as a result of continuous meshing of the gear teeth. The gear mesh stiffness in this study was determined by assuming the gears to be elastic bodies while modelling the contacts between them. This was followed by performing a stationary time analysis to determine the gear mesh stiffness for different point of contacts in the mesh cycle which practically is the rate of gear rotation after which, the next tooth occupies the position of the first one.

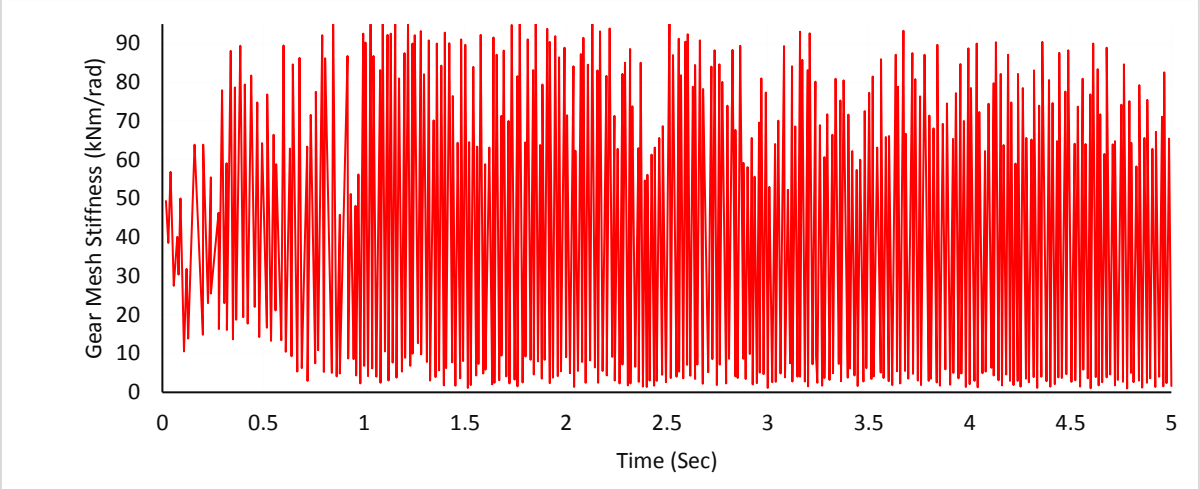

Fig. 2. *Plot of gear mesh stiffness against time.*

Angular velocity of the gear system is the rate of velocity at which the planetary gear rotates around a centre or specific point in a given time interval. As shown in Fig. 3, the angular velocity at the second stage input shaft was plotted against the analysis real time. The plot indicates that at low rotation speed and low time sequence, an increase from 0-2000 RPM was observed in the angular velocity within time sequence of 0-1 second. This was followed by sinusoidal variation of the angular velocity as the analysis time increased. The magnitude of angular velocity is the angular speed of the gear train as it rotates about a specified axis in radians per second. The said angular speed can affect the gear performance if operated at very high velocities. Uematsu [10] investigated the effect of variation of angular velocity in gear rolling process on profile error. The result revealed that the variation of angular velocity is based on the rolled profile error. In other words, amplitude of the variation corresponded with the difference in the rate of plastic deformation between the driven and the follower side of the rotating gear teeth.

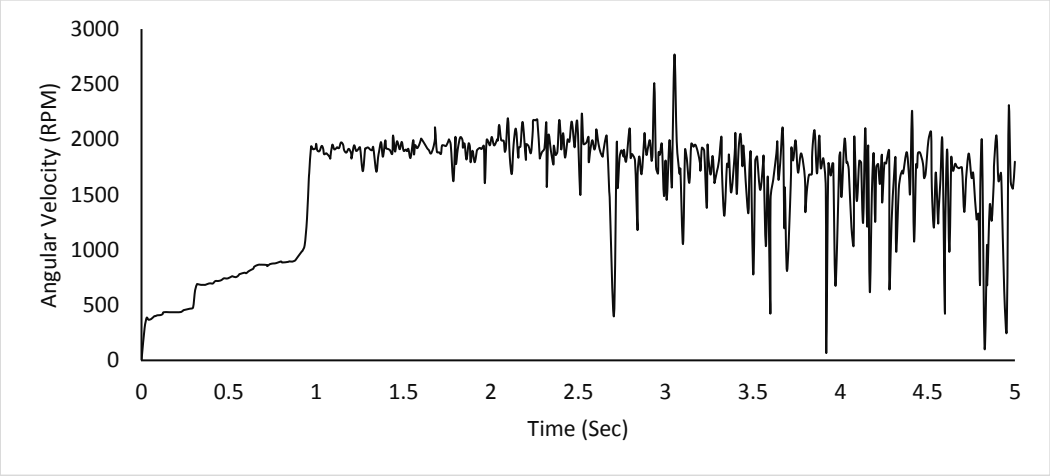

Fig. 3. *Plot of angular velocity against time.*

Generally, torque is the driving force produced by the planetary gear output shaft or the force exerted by the output shaft during rotation, and increases depending on the gear ratio. However, electrical power generated from a wind turbine system depends directly on the rotational speed of the wind turbine blade which via a connecting shaft transfers the high speed momentum generated during rotation to the gearbox for effective control of the input speed (in terms of the input force on the rotating shaft) and

transmission of the required output torque to electric motor for power generation. Fig. 4 represents a plot of motor torque against time. In practical sense, there is a relationship between the motor torque and the speed of the turbine rotor blades, as increased speed of the rotor blade can impact more momentum on the rotating shaft and vice versa. The increased or decreased momentum which impact on the rotating shaft to deliver high or low torque is graphically represented in Figure 4 as a function of time.

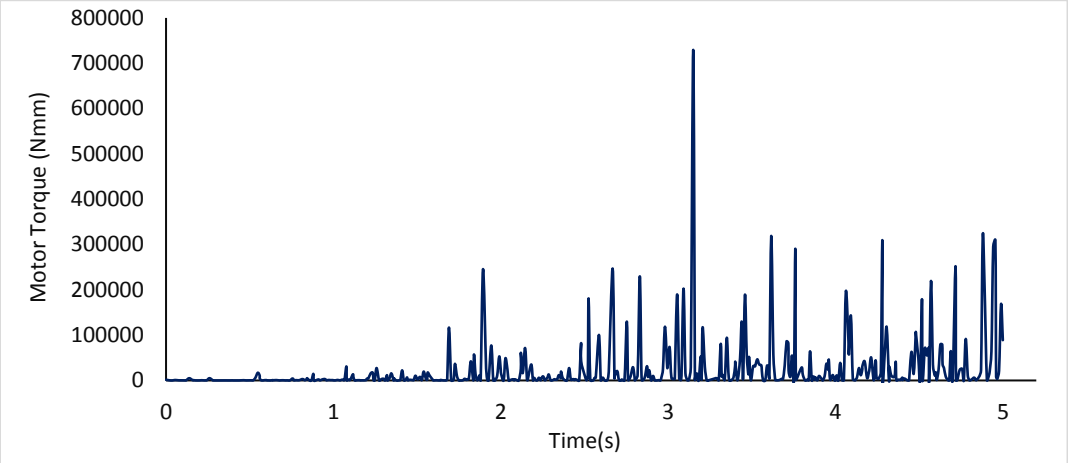

Fig. 4. *Plot of motor torque against time.*

As contact point is established during meshing of the two rotating gear members with one another, contact force which is equal and opposite across the interface between the sun and planet gears is produced. In other words, the said contact force is tangential to both gears and produces a torque that is equal to the radius times the force. As shown in Fig. 5, the contact force changes between the gear tooth flanks at every instant time of the gear rotation cycle. Investigation carried out by Do et al. [11] revealed that at contact force of about 200 Nm and 400 Nm, the contact forces increases which led to larger elastic deformations, increasing tooth bending deformation as well as larger backlash between the meshing gear teeth. While the investigation revealed that the elastic deformation influences the gear transmission ratio and accuracy of transmission, contact force oscillations which were also observed are caused by the change of number of interacting teeth during meshing, indicating the higher contact force is also responsible for higher oscillation. Contact force of 100 Nm was considered to have a mild effect while contact force of 20 Nm was observed have very little effect on the gear tooth.

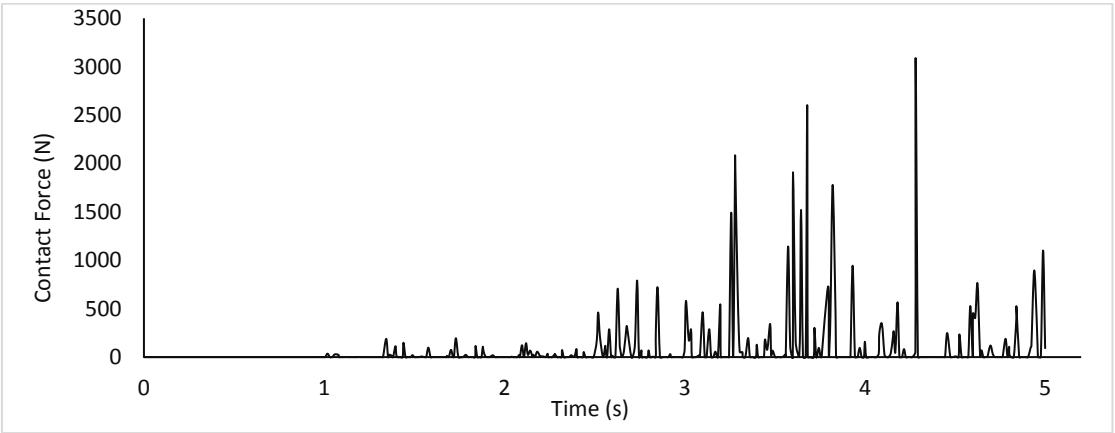

Fig. 5. *Plot of contact force between sun gear and planet gear against time.*

Wind turbine system is designed to operate with three (3) categories of wind speed including cut-in wind speed where the rotor blade does not rotate effectively and falls in the range of 3 and 4 m/s, rated wind speed where the rotor blade rates optimally and falls in the range of 11-15 m/s and cut-out wind speed where the rotor blade rotates beyond optimum speed in the range of 20-24 m/s. [12]. The rotors while operating under cut-out wind speed range oftentimes shutdown to avoid damages to the gear system and other operating components. However, as the rotor blades rotates at higher and lower speeds and drive the gear system, internal forces due to vibration and cyclic loading also set in as the gear tooth members contact with one another. These forces can incite stresses and strains on the gear material and other operating components. Depending on the severity of forces acting on the material, deformations may ensue, indicates the amount of failure in the gear system when it undergoes a certain degree of vibrational excitation during rotation. In this study, rotation magnitude of 120 rpm was employed in simulating the planetary gear for five (5) steps at 2.5 seconds each using Finite Element Method (FEM). To minimize the level of deformation on a given material under such operational condition, Factor of safety (FOS) which is the ratio of ultimate strength of the planetary gear member to the actual working stress or maximum permissible stress of the planetary gear in service condition may be considered as shown in Figure 6a.

From the colour distribution profile of the simulated gear model in Fig. 6, FOS between 0.0116 and 1.0 which are designated by red and FOS between 1.0 and 5.0 which are designated by orange colour are too low which indicates that designing the planetary gear members with FOS in this range is not safe and may expose the gear to limited design life or untimely failure during working condition. This agrees with the findings of Ikpe et al. [13] where FEM was also used in their investigation. From the colour distribution profile in Figure 6, areas with FOS between 5.0 and 10.0 is designated by lemon colour which implies that the gear members are most likely safe, whereas, FOS between 10.0 and maximum FOS value of 15.0 designated by royal blue colour indicates that designing the planetary gear members with FOS in the range of 10.0 and 15.0 is safe and can withstand high stress and strain defects on the gear members during service condition. Hence, the higher the FOS value selected for a given design, the higher the performance of the component in terms of strength and resistance against its in-service loading condition and the higher its manufacturing cost [14]. It should be noted in the colour profile for all the simulated gear models in this study that the royal blue colour signifies minimum severity for any parameter represented while the red colour signifies maximum severity. While centrifugal force is generated during rotation, the gear rotor wheels rotating about a fixed point is balanced by the force of gravity which is proportional to the centrifugal force. The standard earth gravity behind this principle is represented in Fig. 6b. Since the motion of the gear wheels is circular, the acceleration force can be calculated as the product of the radius and the square of the angular velocity.

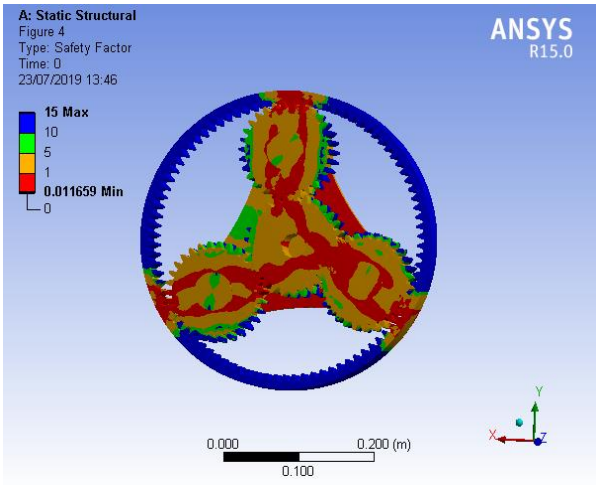

Fig. 6(a). *Profile showing safety factor of the gear model.*

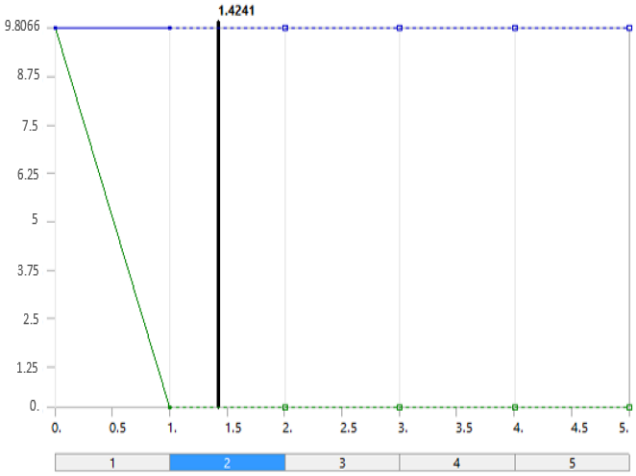

b.

Fig. 6(b). *Standard earth gravity of the gear rotor wheels.*

Fig. 7a represents the equivalent Von-misses stress profile while Fig.7b is a graphical representation of the same Von-mises stress components resulting from the dynamics of the planetary gear during rotation. In the simulation, the ring gear was considered as statically constrained member because it is practically fixed to the gearbox housing while the dynamics of the planet gear, planet carrier and the sun pinion were considered as rotating members about an axis. The simulation which was conducted for five (5) steps at 2.5 seconds each yielded minimum and maximum Von-mises stress of 10.168 Pa and 5.9889e+009 Pa for the 5th step. To determine the severity of the Von-mises stress values on the simulated planetary gear system, the colour distribution profile on the model was evaluated. In the case of FOS shown earlier in Figure 6, royal blue colour represented maximum FOS which indicated that a given design with FOS of such value is safe, whereas, red colour represented minimum FOS which indicated that a given design with FOS of such value is prone to failure [15]. For the static structural analysis presented in Figure 7a, royal blue colour represents minimum Von-mises stress which indicates that a given design with such stress value is safe while red colour represents maximum stress value which indicates that a given design with such stress value is prone to failure. Thoroughly observing the colour distribution profile across the simulated planetary gear model in Fig. 7a, it can be observed that royal blue colour is dominant with traces of light green on the meshing point between the planet gear and sun gear. This signifies that a given 2-stage planetary gear that is designed and operated under the

aforementioned conditions and FOS is likely to perform optimally and as well meet its expected design life.

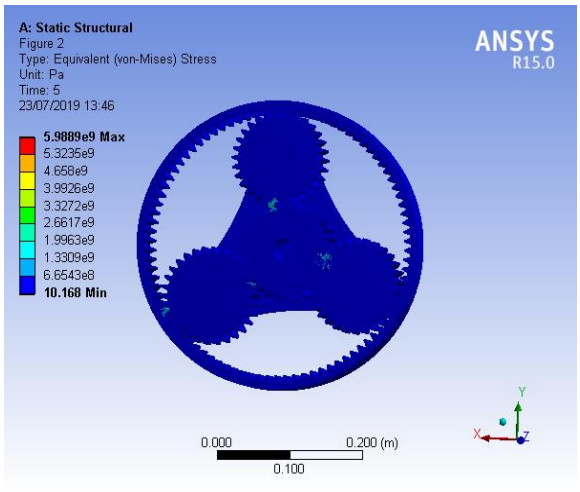

Figure 7(a). *Equivalent stress profile from static analysis.*

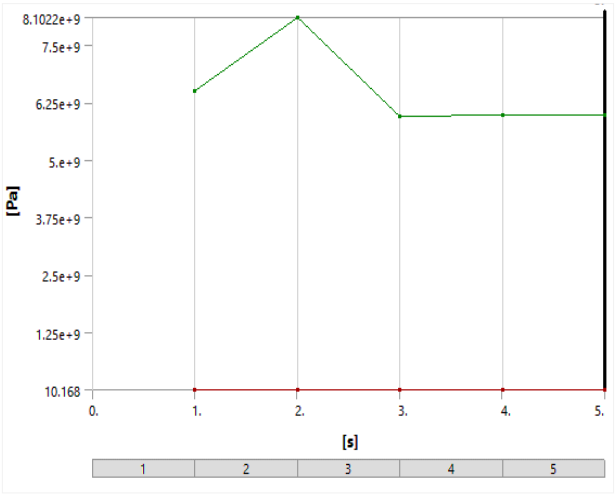

Fig. 7(b). *Plot of equivalent stress from static analysis.*

Fig. 8a represents the equivalent elastic strain profile while Fig. 8b is a graphical representation of the said elastic strain components resulting from the dynamics of the planetary gear during rotation. The simulation which was conducted for five (5) steps at 2.5 seconds each yielded minimum and maximum equivalent elastic strain of 5.0839e-011 and 2.9944e-002 for the 5th step. Using the colour profile explanation in Figure 8a to determine the severity of the equivalent strain values on the simulated planetary gear model, it can also be observed that royal blue colour is dominant with traces of light green on the meshing point between the planet gear and sun gear. This signifies that a given 2-stage planetary gear that is designed and operated under the aforementioned conditions and FOS is likely to perform optimally in service condition. When the planetary gear material is exposed to external and internal forces due to vibration of the wind turbine at higher and lower frequency cycles stress is induced in the material which eventually translates into deformation as a result of strain. In this case, strain is the response of the gear material to induced stress/force at each rotation cycle made by the interlocking gear members. In other words, it is the amount of deformation in the direction of induced stress divided

by the original geometry of the reference planetary gear system. The said deformation can be considered elongations due to distortion of atoms within the metal or material, and are dependent on the axis of measurement [13, 16].

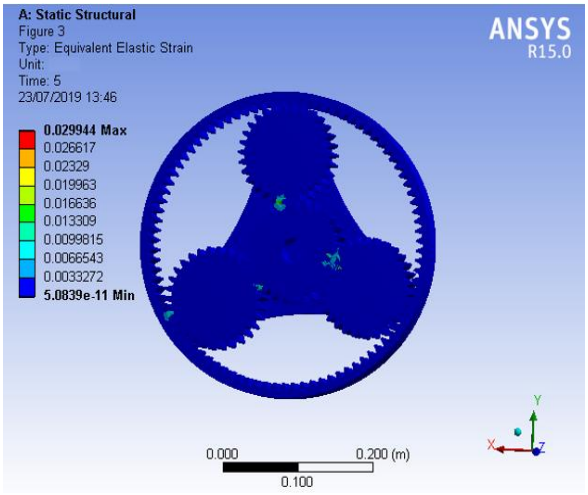

Fig. 8(a). *Equivalent elastic strain profile from static analysis.*

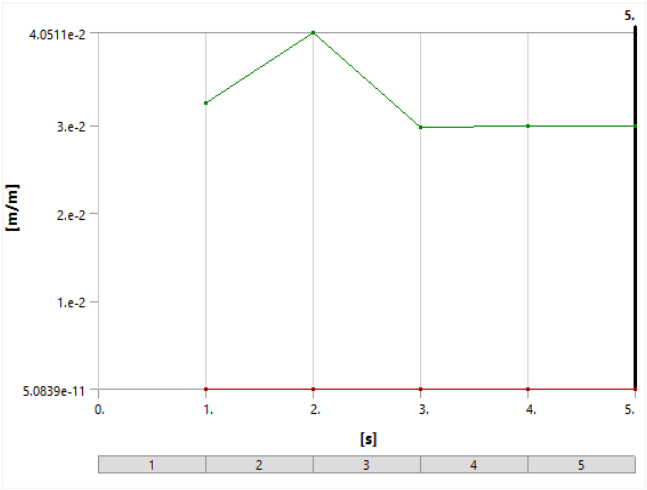

Fig. 8(b). *Plot of equivalent elastic strain from structural analysis.*

Fig. 9a represents the total deformation profile while Fig. 9b is a graphical representation of the total deformation resulting from the aforementioned stress and strain component of the planetary gear during rotation. As shown in Figure 9a, the maximum total deformation of 1.7318e-003 m was obtained at the 5th step of the five (5) steps simulation conducted for 2.5 seconds each. From the colour distribution on the simulated planetary gear model in Figure 9a, deformation can be observed to be more severe on the sun and planet gear meshing tooth indicated by red colour. This is as a result of the contact force and interplay between the sun and planet gear. In a typical gear tooth application, the gear tooth deformation may occur in the form of wear rate which can translate into gear tooth mesh problems, thereby, causing the rotating gear member to suddenly hook during operation. This can affect the transmission ratio of the gear and also cause vibrational excitations at high frequencies which may result in misalignment of the gear shafts and other operating members of the system. Studies have shown that one of the ways of mitigating against unwanted gear tooth wear is through lubrication which provides an oil-protecting film to the meshing gear tooth surface and also reduces the frictional force acting between the meshing

gear tooth [17], thereby, making it easy for the gear to transmit torque to the wind turbine electric motor for effective power delivery. The equivalent von-mises stress, equivalent strain as well as the total deformation resulting from the in-service condition of the 3-stage planetary gear analysed in this study is presented in Table 4.

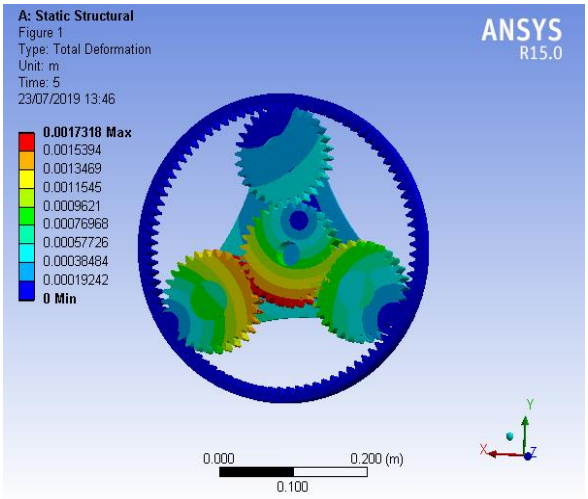

Figure 9(a). *Profile showing Total deformation from static analysis.*

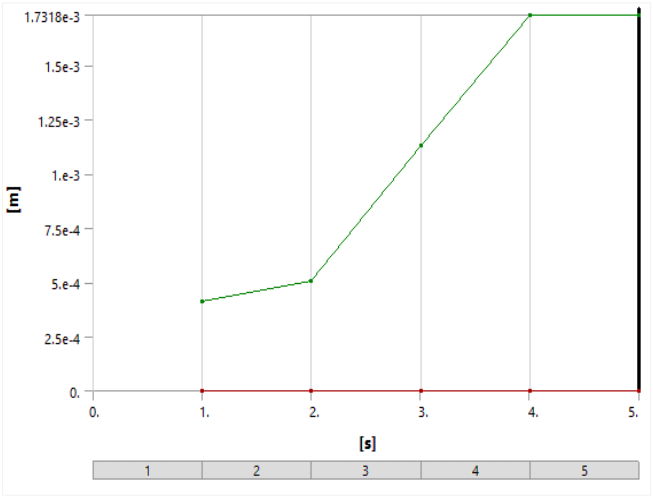

Fig. 9(b). *Graph of total deformation from static analysis.*

Table 4. *Total deformation from static analysis.*

Time (s)	Equivalent Stress		Equivalent Elastic Strain		Total Deformation	
	Minimum (Pa)	Maximum (Pa)	Minimum	Maximum	Minimum (m)	Maximum (m)
1	*10.294*	*6.4981e+009*	*5.1471e-011*	*3.249e-002*	*0*	*4.1016e-004*
2	*10.292*	*8.1022e+009*	*5.1462e-011*	*4.0511e-002*	*0*	*5.0565e-004*
3	*10.22*	*5.9398e+009*	*5.1099e-011*	*2.9699e-002*	*0*	*1.1287e-003*
4	*10.168*	*5.9831e+009*	*5.0839e-011*	*2.9916e-002*	*0*	*1.7316e-003*
5	*10.168*	*5.9889e+009*	*5.0839e-011*	*2.9944e-002*	*0*	*1.7318e-003*

4. Conclusion

In this study, a 2-stage planetary gear train applicable to modular horizontal wind turbine has been successfully modelled and analysed to determine its in-service performance. The analysis which encapsulated failure modes such as equivalent stress, strain and total deformation indicated that the selection of high FOS, for example 10 and above can greatly minimise the effects of the aforementioned failure modes and optimise operation efficiency and service life but at the expense of manufacturing cost. It was also found that, higher contacting forces along the meshing gear tooth can incite stresses and deformations that may eventually translate into gear tooth failure as well as low gear transmission ratio/torque. Moreover, the planetary gear mesh stiffness must be maintained at low level through adequate lubrication to reduce high contact forces and enable the interlocking gear teeth mesh with ease. The analysis in this report serves as a guideline for better understanding of the operation cycle of a planetary gear.

References

[1] Filiz, İ. H., Olguner, S., & Evyapan, E. (2017). A study on optimization of planetary gear trains. *Acta physica polonica, A.*, *132*(3).

[2] Ragheb, A., & Ragheb, M. (2010, March). Wind turbine gearbox technologies. *2010 1st international nuclear & renewable energy conference (INREC)* (pp. 1-8). IEEE.

[3] Cooley, C. G., & Parker, R. G. (2014). A review of planetary and epicyclic gear dynamics and vibrations research. *Applied mechanics reviews*, *66*(4).

[4] Höhn, B. R., Stahl, K., & Gwinner, P. (2013). Light-weight design for planetary gear transmissions. *Gear technology*, *9*, 96-103.

[5] Hamand, Y. C., & Kalamkar, V. (2011). Analysis of stresses and deflection of sun gear by theoretical and ANSYS method. *Modern mechanical engineering*, *1*(02), 56.

[6] Pawar, P. V., & Kulkarni, P. R. (2015). Design of two stage planetary gear train for high reduction ratio. *International journal of research in engineering and technology*, *4*(06), 150-157.

[7] JGMALR, J. F. M. (2009). *Wind energy explained: theory. design and application, 2nd Edition*, Massachussets: Wiley.

[8] Norton, R. L. (2006). *Machine design: an integrated approach, 3rd edition*. Upper Saddle River, NJ: Pearson Prentice Hall.

[9] Schulze, T., Hartmann-Gerlach, C., & Schlecht, B. (2010, October). Calculation of load distribution in planetary gears for an effective gear design process. In *AGMA fall technical meeting* (pp. 17-19).

[10] Uematsu, S. (2002). Effect of variation of angular velocity in gear rolling process on profile error. *Precision engineering*, *26*(4), 425-429.

[11] Do, T. P., Ziegler, P., & Eberhard, P. (2017). Simulation of contact forces and contact characteristics during meshing of elastic beveloid gears. *Computer assisted methods in engineering and science*, *21*(2), 91-111.

[12] Huso, M. M., & Hayes, J. P. (2009). *Effectiveness of changing wind turbine cut-in speed to reduce bat fatalities at wind facilities*. Retrieved from https://www.researchgate.net/profile/Manuela_Huso/publication/253970541_Effectiveness_of_Changing_Wind_Turbine_Cut-in_Speed_to_Reduce_Bat_Fatalities_at_Wind_Facilities/links/548f2c7d0cf214269f26376d.pdf

[13] Essienubong, I. A., Ikechukwu, O., & Ebunilo, P. O. (2016). Determining the accuracy of finite element analysis when compared to experimental approach for measuring stress and strain on a connecting rod subjected to variable loads. *Journal of robotics, computer vision and graphics*, *1*(1), 12-20.

[14] Ikpe, A., & Owunna, I. (2019). Design of remotely controlled hydraulic bottle jack for automobile applications. *Uluslararası mühendislik araştırma ve geliştirme dergisi*, *11*(1), 124-134.

[15] Ikpe, A. E., Orhorhoro, E. K., & Gobir, A. (2017). Design and reinforcement of a b-pillar for occupants safety in conventional vehicle applications. *International journal of mathematical, engineering and management sciences*, *2*(1), 37-52.

[16] Ikpe, A. E., & Owunna, I. (2017). Design of vehicle compression springs for optimum performance in their service condition. *International journal of engineering research in Africa*, *33*, 22-34.

[17] Ștefănescu, T. M., Volintiru, O. N., & Scurtu, I. C. (2018, November). Considerations regarding the lubrication of Marine Gearboxes. *Journal of physics: conference series* (p. 012025). IOP Publishing.